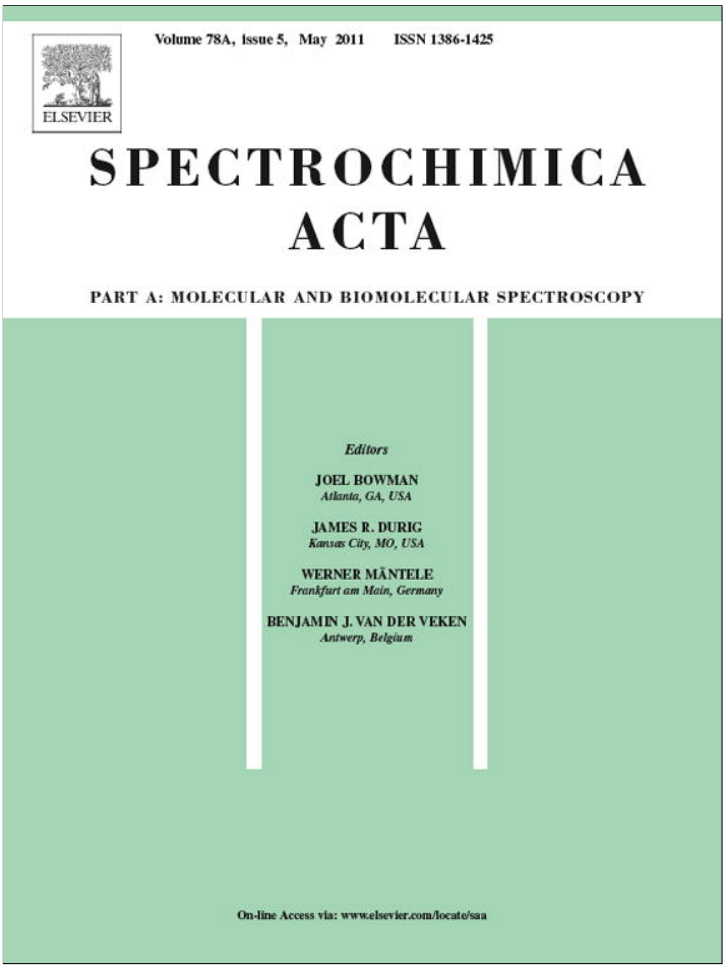

Spectrochimica Acta Part A 78 (2011) 1376–1379

Contents lists available at ScienceDirect

Spectrochimica Acta Part A: Molecular and Biomolecular Spectroscopy

journal homepage: www.elsevier.com/locate/saa

Vibrational analysis of 1-methyl-pyridinium-2-aldoxime and 1-methyl-pyridinium-4-aldoxime cations

Vlasta Mohaček Grošev[a,*], Blaženka Foretić[b], Ozren Gamulin[c]

[a] Ruđer Bošković Institute, Bijenička 54, POB 180, 10002 Zagreb, Croatia
[b] Department of Chemistry and Biochemistry, Faculty of Medicine, University of Zagreb, Šalata 3, 10000 Zagreb, Croatia
[c] Department of Physics and Biophysics, Faculty of Medicine, University of Zagreb, Šalata 3, 10000 Zagreb, Croatia

ARTICLE INFO

Article history:
Received 26 March 2010
Received in revised form 13 January 2011
Accepted 17 January 2011

Keywords:
1-Methyl-pyridinium-2-aldoxime chloride
1-Methyl-pyridinium-4-aldoxime chloride
Normal coordinate analysis
Infrared
Raman

ABSTRACT

Pyrimidinium aldoximes are administered intravenously in cases of acute organophosphate poisoning. Since questions regarding their morphology and active conformation in the solution are still open, an effort was made to establish correspondence between their crystal state conformers and vibrational spectra, thus facilitating the future work on the assignment of bands in solution.

Normal coordinate analysis including the potential energy distribution for all modes was performed for 1-methyl-pyridinium-2-aldoxime (PAM2AN) and 1-methyl-pyridinium-4-aldoxime (PAM4AN) cations (charge = +e, spin = 0). Positions of infrared and Raman bands of corresponding chloride salts agree rather well with predicted values, except for modes taking part in hydrogen bonding to anions. The strength of hydrogen bonding is estimated to be of medium strength in both salts, the bonding in PAM2AN being stronger. The calculated and observed values of the characteristic stretching modes for the aldoxime moiety have been in accordance with the stronger acidity of PAM2AN structural isomer.

1. Introduction

Pyrimidinium aldoximes are used as antidotes for acute organophosphate poisoning, during which acetylcholinesterase (AChE) is irreversibly inhibited and death occurs in a matter of minutes [1]. Both insecticides and chemical warfare agents contain an invasive phosphate group that binds to the catalytic site of AChE – that is reacts with hydroxyl group of the Serine 200 – burried in a 20 Å deep and 6 Å wide gorge [2]. Reactivation of the inhibited enzyme is hampered by its "ageing", an autocatalytic process whereby enzyme loses its active oxygen together with an alkyl chain tied to the organophosphate [3]. The most potent and universal antidote would have to bind to the phosphate group, and remove it from the enzyme but without destructive consequences.

AChE active site catalyses the hydrolytic cleavage of acetylcholine into an acetate CH_3COO^- and a choline $HO–CH_2CH_2N^+(CH_3)_3$. When the active site is tied to a phosphorous group, enzyme is disabled and acetylcholine agglomerates, causing paralyses of muscles. Further aggravation is caused by enzyme ageing, when serine oxygen leaves the enzyme together with the phosphate group. The mono- and bis-pyridinium type aldoximes are used as reactivators of non-aged AChE. The bis-pyridinium aldoxime salts (e.g. HI-6, obidoxime, TMB-4) are found to be more potent than mono-pyridinium aldoximes such as 1-methyl-pyridinium-2-aldoxime (PAM2AN) and 1-methyl-pyridinium-4-aldoxime (PAM4AN), although the chloride or iodide salts of PAM2AN known as pralidoxime do have pharmacological application [1]. Stability and reactivity (nucleophilicity and reactivation ability) of pyridinium aldoximes is closely related to their morphology, configuration and conformation, which also determines the acidity of aldoxime group. The configuration of aldoxime group and consequently its acidity and nucleophilicity in such compounds are known to vary with temperature or upon UV irradiation [4–6].

Since the question regarding the morphology and active conformation of a solid simple mono-pyridinium aldoximes is still open [7], and since at physiological pH (7.4) oxime group exists both in protonated and in deprotonated forms [6], one could gain much information by studying the pyridinium aldoxime solution vibrational spectra. Therefore the first step would be to assign the vibrational bands of the protonated conformers appearing in crystals. The crystal structure of pralidoxime (PAM2AN, chloride salt) is known [8], but data is still missing for PAM4AN chloride. It is therefore of interest to establish a correspondence between structure and vibrational spectra of these physiologically active molecules.

2. Materials and methods

The white to pale yellow crystalline solids of 1-methyl-pyridinium-2-aldoxime (PAM2AN) and 1-methyl-pyridinium-4-

* Corresponding author. Tel.: +385 1 4561 020; fax: +385 1 4680 112.
E-mail address: mohacek@irb.hr (V.M. Grošev).

1386-1425/$ – see front matter © 2011 Elsevier B.V. All rights reserved.
doi:10.1016/j.saa.2011.01.012

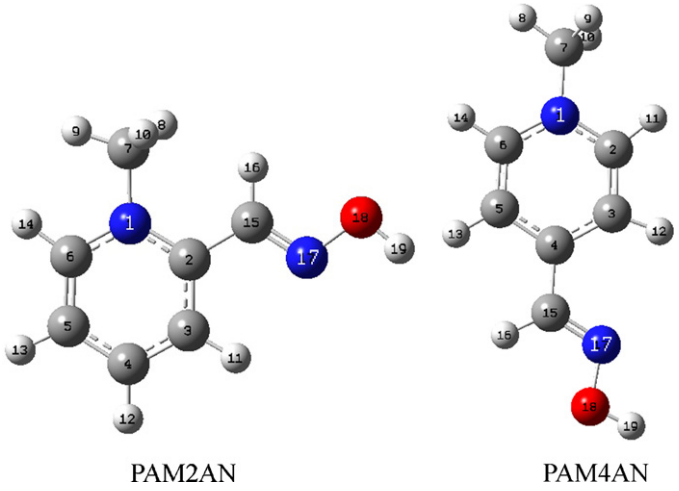

Fig. 1. The most stable conformation of *E*-anti-anti PAM2AN (left) and of *E*-syn-anti PAM4AN (right) (charge = +e, spin = 0). Selection of optimized geometrical parameters is given in Table 1 for PAM2AN, and in Supplementary Table S1 for PAM4AN.

aldoxime (PAM4AN) chlorides were commercial substances synthesized by known methods [9] (manufactured by Bosnalijek) and used as supplied.

Raman spectra of powdered samples pressed into spherical hollow holders were recorded with FT-Raman module of Perkin-Elmer GX spectrometer in spectral range from 150 to 3500 cm^{-1} with resolution of 1 cm^{-1} and accumulation of 500 scans. The excitation line was $\lambda = 1064$ nm of Nd:YAG laser operating at the power of 300 mW, with InGaAs detector. Infrared spectra of powdered samples pressed in KBr pellets were recorded in transmission mode by Perkin-Elmer GX spectrometer, equipped with DTGS detector, in absorption mode with 150 scans and 1 cm^{-1} resolution. Spectral range was from 370 to 4000 cm^{-1}.

3. Results and discussion

Normal modes of PAM2AN and PAM4AN cations in *E* configuration were calculated and compared with observed Raman and infrared bands of their chloride salts. The *E* configuration for the arrangement of substituents around the C=N bond has been found in all other oximes with antidotal activity against intoxication with organophosphate poisons [7,8]. Based on the known crystal structure of PAM2AN [8] the Raman and infrared bands could be assigned according to their symmetry. The agreement was rather good, except for modes reflecting changes due to hydrogen bonding to chloride anion. The assignment of the bands for PAM4AN, whose crystal structure is unknown, was done by comparison with calculated cation normal vibrations.

Comparing the optimized geometry for the *E*-anti-anti conformer of PAM2AN cation (Fig. 1, left) with the crystal structure parameters (Table 1), we have found that they were qualitatively the same, but calculated lengths of bonds in the pyridinium ring are systematically longer than the ones found in the crystal. The exception in that trend was found for the aldoxime N–O bond whose calculated length was slightly shorter indicating strong resonance interaction between the pyridinium ring and the aldoxime moiety. Considerable contribution of =C–N=O^+H resonance structure has been found in the crystal structure of several PAM2AN salts [8] and is in accordance with the higher acidity of the pyridinium-2-aldoximes in comparison with their 4-substituted isomers [10]. Moreover, it was also established by the calculated charge separation in the aqueous phase [7]. Selections of optimized parameters for PAM4AN cation is given in Table S1, Supplementary material.

Table 1
Comparison of selected geometrical parameters for *E*-anti-anti conformer of PAM2AN calculated with B3LYP/6-31++G(d,p) method [12] with the crystal structure parameters [8].

	B3LYP	Crystal
Bonds (Å)		
N1–C2	1.371	1.352
C2–C3	1.403	1.386
C3–C4	1.387	1.365
C4–C5	1.401	1.377
C5–C6	1.379	1.357
C6–N1	1.362	1.352
N1–C7	1.486	1.474
C2–C15	1.462	1.460
C15–N17	1.288	1.274
N17–O18	1.359	1.372
Angles (°)		
C2–C15–N17	117.70	116.94
C15–N17–O18	111.82	111.77
Dihedrals (°)		
N1–C2–C3–C4	0.0	1.51
C2–C3–C4–C5	0.0	0.18
C3–C4–C5–C6	0.0	−1.73
C4–C5–C6–N1	0.0	1.61
C5–C6–N1–C2	0.0	0.12
C6–N1–C2–C3	0.0	−1.66
C3–C2–C15–N17	−0.01567	−7.6

The most stable conformation of PAM2AN cation was the *E*-anti-anti form, while the *E*-syn-anti cation form was 0.44 kcal/mol higher in energy. The conformation notation refers to the dihedral angles N1–C2–C15–N17 and C2–C15–N17–O18 (Fig. 1), and has been found as the most stable optimized one for PAM2AN chloride [7,11].

Crystal structure of PAM2AN chloride belongs to $P\bar{1}$ space group with two molecules per unit cell ($Z = 2$), $a = 7.110$ Å, $b = 7.165$ Å, $c = 8.861$ Å, $\alpha = 76{,}52°$, $\beta = 85{,}62°$, $\gamma = 65{,}8°$ [8]. There are 117 optically active phonons, 60 of A_g and 57 of A_u symmetry. Among 60 A_g Raman active modes, 6 belong to librations of PAM2AN cations in the rigid molecule approximation, 51 to internal vibrations of PAM2AN cations and 3 describe hydrogen bonding of cations to chloride anions. Fifty-seven infrared active modes comprise 6 translations of cations and Cl^- anions, and the other 51 modes belong to internal vibrations of PAM2AN cations. Since only internal part of vibrational spectrum is of interest here, low frequency spectra were not recorded.

In Table 2 selection of observed Raman and infrared modes for PAM2AN chloride crystal is listed and compared with the calculated values for PAM2AN cation (charge = +e, spin = 0) using Gaussian 03 program [12], while complete list of all observed and calculated bands is given in Table S2, Supplementary material. From the output log file we created the input file for the MOLVIB program of Kuczera [13] and found the potential energy distribution. The same procedure was performed for PAM4AN (Fig. 1, right) and the selection of results is given in Table 3, while complete list of all bands in Table S3, Supplementary material. The infrared and Raman spectra of two compounds are shown in Figs. 2 and 3.

We have been concentrated on several aldoxime group modes that most likely experienced shifts and/or broadening in a crystal upon hydrogen bonding to chloride anion, and whose position revealed the acido-basic properties of the examined structural isomers.

3.1. OH stretching

In the infrared spectrum of PAM2AN chloride, O···Cl^- distance equals to 2.988 Å [8] and O–H stretching band has been attributed to the broad band centered around 2800 cm^{-1} underlying $-CH_3$ and $C-H_{ring}$ stretching bands. This value is close to

Table 2
Positions of selected observed Raman and infrared bands compared to calculated unscaled frequencies of normal modes of E-anti-anti conformer of pralidoxime (1-methyl-pyridinium-2-aldoxime-chloride) (cm^{-1}). In calculation, the geometry of 1-methyl-pyridinium-2-aldoxime ion was optimized using B3LYP/6-31++G(d,p) method.

Observed		Calculated			Potential energy distribution (%)
Raman crystal A_g	Infrared crystal A_u	calculated value	Raman scattering activity (10^{-40} m^4/a.m.u.)	Infrared intensity (KM/mol)	
1631 mw	1640 w, sh 1629 m	1681	11	34	28 ν(C=N_{oxim}) + 22 ν(C=C) + 14 ((C_{ring}–C_{ring}) + 10 ((C_{ring}–H)
1599 vs	1629 m 1596 m, sh	1649	369	95	46 ν(C=N_{oxim}) + 19 ((C_{ring}–H) + 10 δ(N–O–H)
1584 s, sh 1105 vw	1582 s 1117 w	1615	96	78	29 ν(C_{ring}–C_{ring}) + 17 ν(C=N_{ring}) + 16 ν(C_{ring}=C_{ring}) + 12 ((C_{ring}–H)
1068 m	1071 vs	1082	2.5	162	35 ν(N_{oxim}–O) + 23 δ_{sym}(CH_3) + 11 ν(C=N_{ring})
1055 m	1051 w	1099	19	114	30 ν(N_{oxim}–O) + 18 δ_{asym}(CH_3) + 12 Φ(C_{ring}–H) + 11 ν(C_{ring}–C_{ring})

Table 3
Positions of selected observed Raman and infrared bands compared to calculated frequencies of normal modes of 1-methyl-pyridinium-4-aldoxime-chloride (cm^{-1}). In calculation, the geometry of 1-methyl-pyridinium-4-aldoxime ion was optimized using B3LYP/6-31++G(d,p) method.

Observed		Calculated			Potential energy distribution (%)
Raman crystal	Infrared crystal	Calculated value	Raman scattering activity (10^{-40} m^4/a.m.u.)	Infrared intensity (KM/mol)	
1676 mw					
	1651 s, sh				
1643 s	1647 s, sh 1639 s 1632 s, sh 1625 mw, sh	1697	34	58	35 ν(C=C) + 18 ν(C=N_{oxim}) + 17 Φ(C_{ring}–H)
1611 vvs	1607 s	1654	634	345	50 ν(C=N_{oxim}) + 10 ν(C=C)
1578 m	1574 w, sh				
1570 m	1568 m	1594	9	19	34 ν(C_{ring}–C_{ring}) + 28 ν(C=N_{ring})
1082 w	1077 w, br	1096	10	143	37 ν(N_{oxim}–O) + 33 δ_{asym}(CH_3) + 12 ν(C=N_{ring})
1051 mw					
1008 m	1009 vs	1074	11	225	43 ν(N_{oxim}–O) + 20 δ_{asym}(CH_3) + 13 ν(C=N_{ring})

the value of ν(OH) calculated by Emmeluth et al. for the phenol complexed with Cl^- at 2815 cm^{-1}, with O···Cl^- distance nearly equal to 2.983 Å [14]. For PAM4AN the centre of gravity of the ν(OH) band is at higher wavenumbers, ~3050 cm^{-1}, which would indicate weaker O–H···Cl^- bonding, and O···Cl^- distance greater than 2.990 Å [11,15]. In the matrix isolation experiment performed by Stepanenko et al. [5] the O–H stretching for the *E*-isomer of electrically neutral, uncharged, pyridine-4-aldoxime, appeared at 3619 cm^{-1} in argon matrix, while Flakus and Michta have discussed the effects of the strong O–H···N hydrogen bonded infinite chains of that molecule in the crystal [16].

3.2. δ(NOH) bending

Two infrared modes of PAM2AN cation have the largest calculated contribution from δ(NOH) (Table S2, Supplementary material). They have been calculated as 1315 cm^{-1} and 1460 cm^{-1} (unscaled). In the experimental infrared spectrum a broad band at 1290 cm^{-1} would correspond to the first mode and a weak band at 1401 cm^{-1} to the second mode. Similar calculated modes at 1304 cm^{-1} and 1452 cm^{-1} have been obtained for PAM4AN, but in the experimental spectrum the band at 1290 cm^{-1} is narrower.

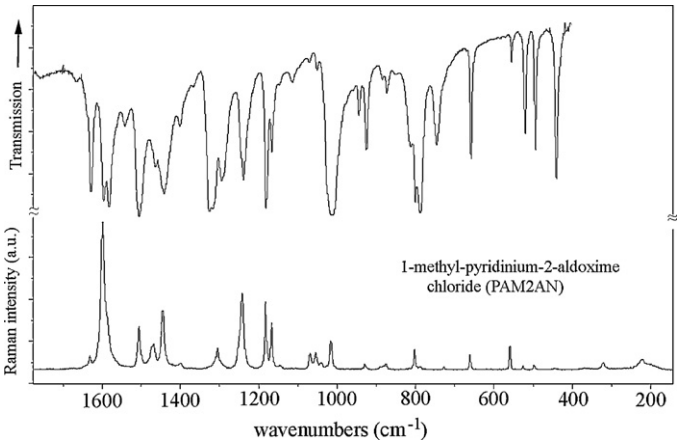

Fig. 2. Comparison of infrared (4000–370 cm^{-1}) and Raman (2000–150 cm^{-1}) spectra of PAM2AN chloride powder.

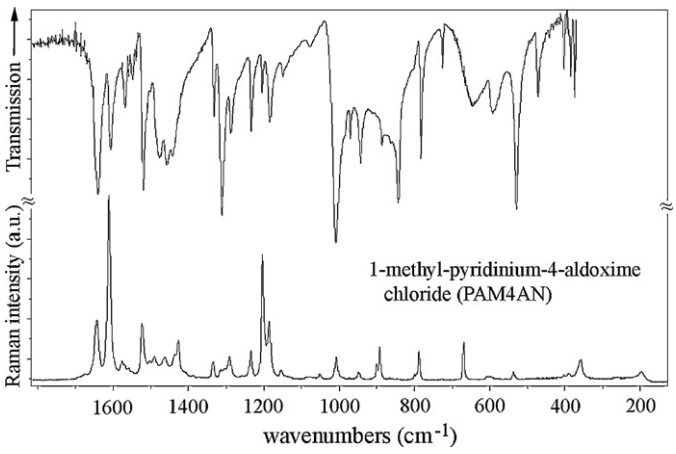

Fig. 3. Comparison of infrared (4000–370 cm^{-1}) and Raman (2000–150 cm^{-1}) spectra of PAM4AN chloride powder.

3.3. ν(N–O) stretching

Both calculated and observed wavenumbers for ν(N–O) has been found to be higher for PAM2AN than for PAM4AN cation. For PAM2AN, ν(N–O) calculated value is at 1082 cm^{-1} and observed at 1071 cm^{-1}, while for PAM4AN the calculated value is at 1074 cm^{-1} and observed at 1009 cm^{-1}. The position of the band clearly indicated the resonance contribution of =C–N=O$^+$H in both structures in comparison with the matrix isolated uncharged pyridine-4-aldoxime whose N–O stretching was assigned to 969 cm^{-1} band [5]. Higher values found for the PAM2AN compared to its 4-structural isomer are in accordance with its higher acidity and consequently enhanced nucleophilic properties at physiological pH.

3.4. τ(OH) torsion

Calculation has predicted torsion of the hydroxyl group at 548 cm^{-1} in PAM2AN, and at 545 cm^{-1} in PAM4AN cation. In PAM2AN chloride crystal spectra, this band is too weak to be observed, but in PAM4AN chloride it can be confidently attributed to the broad infrared band at 647 cm^{-1}.

3.5. ν(C=$N_{aldoxime}$) stretching

This stretching coordinate has been found by normal coordinate analysis to contribute most to two Raman active modes: the first one at 1649 cm^{-1}, and the second one at 1681 cm^{-1} (PAM2AN) or to 1654 cm^{-1} and 1697 cm^{-1} (PAM4AN). The observed bands in the Raman spectra lie at lower wavenumbers: at 1599 cm^{-1} and 1631 cm^{-1} (PAM2AN) and at 1611 cm^{-1} and 1643 cm^{-1} (PAM4AN). In the experimental infrared spectrum the band at 1629 cm^{-1} for PAM2AN and the band at 1607 cm^{-1} for PAM4AN has been undoubtedly assigned to the C=N stretching. The trend that both calculated and observed values for PAM2AN are lower than for PAM4AN indicated again that PAM2AN isomer is stronger acid.

4. Conclusion

The fact that ν(N–O) stretching band and δ(NOH) bending mode associated with aldoxime group appeared at higher wavenumbers in PAM2AN than in PAM4AN indicate stronger hydrogen bonding in PAM2AN chloride than in PAM4AN salt. We estimate the $Cl^-\cdots O$ distance in PAM4AN as being smaller than the value found in PAM2AN chloride: 2.988 Å. These hydrogen bonds strengthen the layer containing anions in PAM2AN chloride crystal, while the forces between layers are somewhat weaker. Weakening of hydrogen bonding in PAM4AN chloride could promote better aqueous solubility of this compound as compared to PAM2AN salt. Higher wavenumbers of ν(N–O) and lower of ν(C=N) stretching modes found for the PAM2AN in comparison to its 4-structural isomer are in accordance with its property of stronger acid and consequently better nucleophilic agent at physiological pH.

The performed band assignment of these crystalline compounds will be very helpful for the future study of their solutions, used in medical applications, in which both protonated and ionized species are present.

Acknowledgements

This work was supported by the Ministry of Science, Technology and Sport of the Republic of Croatia, Grants no. 098-0982904-2898, 108-1193079-3070 and 108-1080134-3105.

Appendix A. Supplementary data

Supplementary data associated with this article can be found, in the online version, at doi:10.1016/j.saa.2011.01.012.

References

[1] F. Worek, L. Szinicz, P. Eyer, H. Thierman, Appl. Pharmacol. 209 (2005) 193.
[2] F. Ekström, M. YSuang-Ping Pang, E. Boman, C. Artursson, S. Akfur, Börjegren, Biochem. Biopharmacol. 72 (2006) 597.
[3] B. Sanson, F. Nachon, J.P. Colletier, M.T. Froment, L. Toker, H.M. Greenblatt, J.L. Sussman, Y. Ashani, P. Masson, I. Silman, M. Weik, J. Med. Chem. 52 (2009) 7593.
[4] F.A. Andrzejevska, L. Lapinski, I. Reva, R. Fausto, Phys. Chem. Chem. Phys. 4 (2002) 3287.
[5] T. Stepanenko, L. Lapinski, M.J. Novak, L. Adamowicz, Vib. Spectrosc. 26 (2001) 65.
[6] B. Foretić, N. Burger, Monatsh. Chem. 135 (2004) 261.
[7] S. Vyas, C.M. Hadad, Chem. Biol. Interact. 175 (2008) 187.
[8] W. Van Havere, A.T.H. Lenstra, H.J. Geise, Acta Cryst. B38 (1982) 2516.
[9] K. Karljiković-Rajić, B. Stanković, A. Granov, Z. Binenfeld, J. Pharm. Biomed. Anal. 6 (1988) 773.
[10] W. Cohen, B.F. Erlanger, J. Am. Chem. Soc. 82 (1960) 3928.
[11] A.T. Castro, J.D. Figueroa-Villar, Int. J. Quant. Chem. 89 (2002) 135.
[12] M.J. Frisch, G.W. Trucks, H.B. Schlegel, G.E. Scuseria, M.A. Robb, J.R. Cheeseman, J.A. Montgomery Jr., T. Vreven, K.N. Kudin, J.C. Burant, J.M. Millam, S.S. Iyengar, J. Tomasi, V. Barone, B. Mennucci, M. Cossi, G. Scalmani, N. Rega, G.A. Petersson, H. Nakatsuji, M. Hada, M. Ehara, K. Toyota, R. Fukuda, J. Hasegawa, M. Ishida, T. Nakajima, Y. Honda, O. Kitao, H. Nakai, M. Klene, X. Li, J.E. Knox, H.P. Hratchian, J.B. Cross, V. Bakken, C. Adamo, J. Jaramillo, R. Gomperts, R.E. Stratmann, O. Yazyev, A.J. Austin, R. Cammi, C. Pomelli, J.W. Ochterski, P.Y. Ayala, K. Orokuma, G.A. Voth, P. Salvador, J.J. Dannenberg, V.G. Zakrzewski, S. Dapprich, A.D. Daniels, M.C. Strain, O. Farkas, D.K. Malick, A.D. Rabuck, K. Raghavachari, J.B. Foresman, J.V. Ortiz, Q. Cui, A.G. Baboul, S. Clifford, J. Cioslowski, B. Stefanov, G. Liu, A. Liashenko, P. Piskorz, I. Komaromi, R.L. Martin, D.J. Fox, T. Keith, M.A. Al-Laham, C.Y. Peng, A. Nanayakkara, M. Challacombe, P.M.W. Gill, B. Johnson, W. Chen, M.W. Wong, C. Gonzalez, J.A. Pople, Gaussian 03, Revision E.01, Gaussian, Inc., Wallingford, CT, 2004.
[13] MOLVIB, program developed by K. Kuczera and J. Wiorkiewicz-Kuczera at Harvard University.
[14] C. Emmeluth, B.L.J. Poad, C.D. Thompson, E.J. Bieske, J. Phys. Chem. A 111 (2007) 7322.
[15] G.A. Jeffrey, An Introduction to Hydrogen Bonding, Oxford University Press, New York, Oxford, 1997.
[16] H.T. Flakus, A. Michta, J. Mol. Struct. 741 (2005) 19.